

# Tradeoff Study of Advanced Transmutation Fuels in Sodium-cooled Fast Reactors

N. E. Stauff<sup>1</sup>, T. K. Kim<sup>1</sup>, S. Hayes<sup>2</sup>

<sup>1</sup>Argonne National Laboratory (ANL), Argonne, U.S.A.

<sup>2</sup>Idaho National Laboratory (INL), Idaho Falls, U.S.A.

*E-mail contact of main author: nstauff@anl.gov*

**Abstract.** Advanced transmutation fuels are being developed for Sodium-cooled Fast Reactors (SFRs) with reduced chemical interaction between the fuel and cladding and higher burnup achievable. Different diluent materials such as Zirconium, MTZ (5Mo-4.3Ti-0.7Zr), with addition of Palladium are considered, together with Cr-coating inside the cladding. The use of advanced transmutation fuels was assessed in this study based on the ABR-1000 concept. This study confirms the significant impact of using advanced transmutation fuels on the reactor physics parameters due to the reduction in heavy nuclei density and to the addition of more absorbing elements. The addition of Palladium leads to increasing the fissile content while decreasing the conversion ratio. The reduced neutron flux in the low-energy range affects the neutronic feedback coefficients by reducing the Doppler effect and increasing the sodium void worth. Using MTZ diluent is also found to affect the reactor physics parameters by requiring higher fissile content, and decreasing the conversion ratio. In this case, however, no significant changes in the feedback coefficients are found despite the large shift in spectrum observed, and caused by the elastic scattering cross-section of Ti-48. A 20  $\mu\text{m}$  coating of Chromium had a minor effect on the reactor physics performance of the SFR.

**Key Words:** SFR, metal fuel, transmutation, coating, Palladium, MTZ.

## 1. Introduction

Metallic fuel was developed and qualified in the EBR-II and FFTF reactors and is currently the preferred fuel option in the U.S. for Sodium-cooled Fast Reactors (SFR). Metallic fuel provides outstanding fuel reliability to high burnup, is compatible with proliferation-resistant electrochemical recycling, it allows compact fabrication processes, and it advantages the inherent safety [1]. In terms of reactor physics, the metal-fueled SFR benefits from a high heavy metal density and a hard neutron spectrum, both effects improving the neutron economy of the reactor.

Under the advanced fuel campaign led by the U.S. Department of Energy, various metallic fuel concepts are being developed mainly targeting the mitigation of fuel cladding chemical interaction (FCCI), the migration of the Lanthanides, and to allow higher burnup [1]. The advanced transmutation fuel concepts proposed include the replacement of the fuel diluent, additives in the fuel slug, and coating at cladding inner surface. These innovative options are proposed to deliver advances in fuel reliability and performance, actinide utilization, while maintaining the benefits of the traditional metallic fuel concept.

Different fuel-diluents and cladding materials might impact the neutronic behavior of a fast reactor by bringing potential absorbent or moderating materials, or by reducing the heavy metal density of the fuel. The changes on the neutron spectrum and on the heavy metal inventory of the SFR can have an impact on some neutronic performance such as the fissile content required, the cycle length, and the neutronic feedback coefficients. In this context, reactor physics calculations were conducted to assess the potential impact advanced

transmutation fuels have on the neutronic behavior of the ABR-1000 Sodium-cooled Fast Reactor concept [2].

### 1.1 ABR-1000 Core Description

The metallic-fueled ABR core concept [2] evaluated in this paper was developed for the study of future fast reactor design options in the United States under the Global Nuclear Energy Partnership (GNEP) program. Compact core concepts with a transuranics (TRU) conversion ratio lower than 1.0 were developed for a one-year cycle length with 90% capacity factor. Conventional or reasonably proven materials were utilized in the ABR core concepts so that the core stays within current fast reactor technology knowledge base. The ABR-1000 core generates 1,000 MW thermal (i.e. ~400 MW electrical), uses U-Pu-10Zr metallic fuel alloy and HT-9 cladding and structural materials. The inlet and outlet sodium temperatures are set to respectively 355°C and 510°C.

Figure 1 shows the radial core layout of the 1,000 MW(th) ABR metallic core. It consists of 180 drivers, 114 radial reflectors, 66 radial shields, and 19 control subassemblies. This core is divided into inner and outer core zones, which are composed of 78 and 102 driver assemblies, respectively. The fuel is managed with a 4-batch U/TRU multi-recycling strategy, using Pu from PWR and DU as external feeds. In this design exercise, a slightly simplified ABR-1000 core configuration was employed and its main assembly parameters are displayed in Table I. The cycle length was set to 370 EFPD for an averaged discharged burnup of 100 GWd/t.

TABLE I. PARAMETERS FOR DRIVER SUBASSEMBLY OF ABR METALLIC CORE (HOT TEMPERATURE).

	Unit	
Overall length of subassembly	cm	397.0
- Lower structure		35.0
- Lower reflector		115.0
- Active core height		85.1
- Replaced bond sodium		20.0
- Gas plenum		92.0
- Upper structure		50.0
Subassembly pitch	cm	16.68
Inter-assembly thickness	cm	0.435
Subassembly duct wall thickness	cm	0.397
Number of fuel pins		271
Outer radius of cladding	cm	0.40
Wire diameter	cm	0.125
Thickness of cladding	cm	0.062
Smear Density	%	75

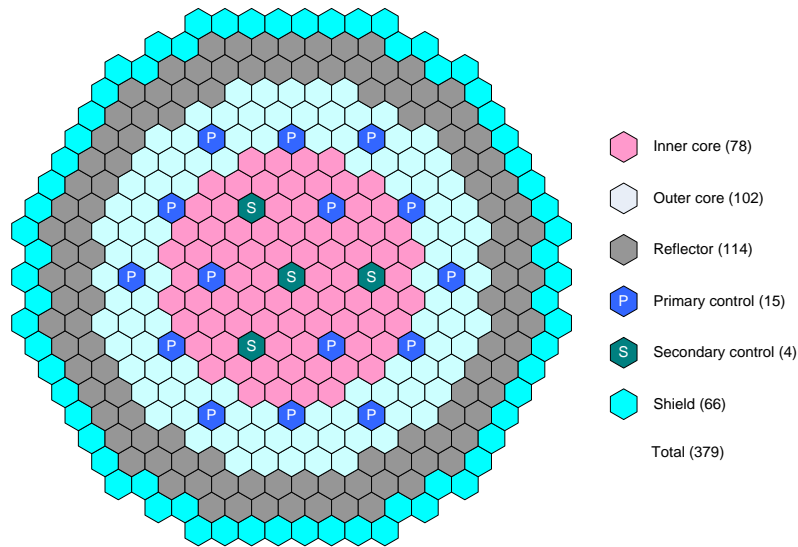


FIG 1. Radial Core Layout of ABR Metallic-Fuel Core.

## 1.2 Advanced Transmutation Fuels

The advanced transmutation fuels investigated in this paper consider the addition of Palladium, the MTZ (5Mo-4.3Ti-0.7Zr) diluent material as a replacement for the traditional 10%Zr, and the Cr coating inside an HT9 cladding [1]. As a consequence, various combinations of the following three fuel options are studied in this section:

- Palladium (Pd) addition in U-Pu-10Zr and U-Pu-MTZ with 2wt% and 4wt% respectively for 10 and 20 at% burnup.
- MTZ (5Mo-4.3Ti-0.7Zr) diluent used as a replacement of 10%Zr.
- Cr coating (20 $\mu$ m at 100% density) inside of an HT9 cladding.

The theoretical fuel and heavy nuclei (HN) densities at room temperature for all investigated fuel options are displayed in Table II. One assumes same density for U and U-Pu transmutation fuels since the Pu-bearing variants of these alloys have not been fabricated yet [3]. Due to the lack of data, the properties of the reference U-Pu-10Zr fuel are being used by default for the swelling, thermal expansion, melting point and thermal conductivity of all transmutation fuels considered.

TABLE II: THEORETICAL DENSITY USED FOR ADVANCED TRANSMUTATION FUELS (ROOM TEMPERATURE).

		U-Pu-10Zr	U-2Pd-10Zr	U-4Pd-10Zr	U-MTZ	U-2Pd-MTZ
Theoretical density	[g/cm <sup>3</sup> ]	15.80	15.79	15.78	14.86	14.71
Theoretical HN density	[g <sub>HN</sub> /cm <sup>3</sup> ]	14.22	13.90	13.57	13.37	12.94

## 1.3 Calculation Methodologies

This analysis was performed using the ANL fast reactor neutronic analysis suite. The suite includes the MC<sup>2</sup>-3 code for generating region-dependent multi-group cross section, the DIF3D code for neutron flux solution, and the REBUS-3 code for depletion analysis.

The MC<sup>2</sup>-3 code [4] is used to calculate the 33-group cross-sections for the REBUS-3 code. MC<sup>2</sup>-3 employs the ENDF/B-VII.0 nuclear data library [5]. Reference homogeneous cross-section calculations employ three steps. The first step uses a fine 2082 energy group structure

and cross sections are condensed into 1041 energy groups. It is followed by a flux calculation step using the 2-D Sn transport solver TWODANT for an approximated cylindrical core with P3 scattering and 1041 energy groups. During the third step, the cross sections are condensed to 33 groups using the flux spectrum integrated over each region with TWODANT.

The whole-core flux calculation is performed with the DIF3D code [6] using diffusion solver for equilibrium calculations or the variational nodal transport solver VARIANT [7] for refined flux calculations with the 33-energy group discretization. Core calculations were done with “all rods out” in a three-dimensional core model where fuel assemblies are radially homogenized. DIF3D is used for calculating neutronic feedback coefficients such as the sodium void worth ( $\Delta\rho_{\text{void}}$ ) and the Doppler constant ( $K_{\text{Dopp}}$ ) using direct calculation.

The REBUS-3 code [8] was used for depletion calculations modeling fuel fabrication, irradiation, discharge cooling, reprocessing, for the equilibrium core analysis. The code was also used for the enrichment search. The cross-sections used for the equilibrium analysis were calculated with MC<sup>2</sup>-3 for the BOC configuration through an iterative process. For equilibrium search, a cooling time and a fabrication time of 1 year were applied to the ABR-1000 core, with 1% of reprocessing losses accounted for.

The Monte Carlo code SERPENT [9] is also employed to verify the accuracy of the deterministic approach employed with the different transmutation fuels. It is a continuous-energy Monte-Carlo reactor physics burnup calculation code developed at the VTT Technical Research Center of Finland. In this analysis, SERPENT is used for detailed core modeling with explicit assembly description, and also employing the ENDF/B-VII.0 nuclear data library.

## 2. Impact of Advanced Fuels on K-effective

This section compares the K-effective results obtained with the deterministic tools of the ANL fast reactor neutronic analysis suite, and with the Monte Carlo solution from SERPENT. The objective is to verify that the deterministic suite provides accurate results when using new types of SFR fuels. The different deterministic assumptions employed in this report are also evaluated with this code-to-code comparison. Three types of fuels are evaluated in this Section: U-Pu-10Zr, U-Pu-2Pd-10Zr, and U-Pu-MTZ, and K-effective results are displayed in Table III. The fuel compositions modeled were obtained by varying the HN density and diluent compositions, but keeping the same isotopic composition of heavy nuclei.

TABLE III: K-EFFECTIVE ESTIMATED WITH DIFFERENT CODES FOR TRANSMUTATION FUELS.

Code Solver	MC <sup>2</sup> -3/DIF3D		SERPENT
	Diffusion	Transport	
U-Pu-10Zr	1.0702	1.0739	1.0817 ± 16 pcm
U-Pu-2Pd-10Zr	1.0446	1.0482	1.0562 ± 16 pcm
U-Pu-MTZ	1.0265	1.0300	1.389 6 pcm

### 2.2 Results of the Code-to-Code Comparison

The results displayed in Table III show the values of K-effective estimated with MC<sup>2</sup>-3/DIF3D using diffusion or transport solvers, and with the SERPENT code. The large variation in K-effective observed from one fuel to the other is the focus of the following paragraph. There is a significant difference between the deterministic and stochastic solutions, since the deterministic diffusion solver consistently under-estimates the k-effective by about

1,000 pcm. The deterministic transport solver provides more accurate results by only 300 pcm, which justifies using the diffusion approximation for the equilibrium search calculations performed in Section 3. The remaining 700 pcm of discrepancy mostly comes from a well-known bias observed when using homogeneous cross-sections in SFR, as reported in Reference [10, 11].

The heterogeneous treatment of the cross-sections available in MC<sup>2</sup>-3 would provide better agreement between the deterministic and stochastic approaches [11]. However, this additional calculation step was neglected for this analysis since the discrepancy observed affects in the same way all types of fuels modeled. In addition, this discrepancy (~1,000 pcm) remains small when compared to the difference in K-effective observed between the different fuel options (2,300 pcm between U-Pu-10Zr and U-Pu-2Pd-10Zr and 3,889 pcm between U-Pu-10Zr and U-Pu-MTZ). Consequently, this code-to-code comparison justifies the use of the deterministic diffusion calculation procedure for conducting the transmutation fuels tradeoff analysis.

## 2.2 Investigation of the Impact of Advanced Fuel on K-effective

The results in Table III show large variations of the K-effective with different transmutation fuels with lower values by 2,300 pcm and 3,889 pcm for the U-Pu-2Pd-10Zr and U-Pu-MTZ fuels, respectively. A breakdown per effect obtained with direct perturbations using DIF3D (diffusion) is displayed in Table III. For complimentary information, Figure 2 shows the neutron flux in the inner core of the SFR using various transmutation fuels, based on the SERPENT solution. Two effects were identified to explain the observed changes in K-effective: the reduction in heavy nuclei density and the changes in diluent and cladding material.

The reduction in the heavy nuclei density plays a large role by reducing the reactivity by 889 pcm and by 2,400 pcm for the U-Pu-2Pd-10Zr and U-Pu-MTZ fuels, respectively. As displayed in Table IV, the effect on the HN density of Pd addition or use of MTZ diluent, is relatively large: for U-Pu-10Zr, the HN density is 14.22 g/cm<sup>3</sup> and it is reduced to 13.9 g/cm<sup>3</sup> with 2%Pd addition, and to 13.37 g/cm<sup>3</sup> with U-Pu-MTZ.

TABLE IV: BREAKDOWN OF THE CHANGES IN K-EFFECTIVE FOR DIFFERENT ADVANCED TRANSMUTATION FUELS OBTAINED WITH DIF3D.

Reference Fuel		U-Pu-10Zr	U-Pu-10Zr
Advanced Fuel Evaluated		U-Pu-2Pd-10Zr	U-Pu-MTZ
Change in HN density	[pcm]	-889	-2400
Pd addition	[pcm]	-1411	
Zr removal	[pcm]		+877
Mo addition	[pcm]		-1651
Ti addition	[pcm]		-653
Total	[pcm]	-2300	-3889

The changes in diluent materials also significantly impact the k-effective as observed in Table IV, due to the different cross-sections (mainly absorption or scattering) from the added elements. For information, Figure 3 displays ENDF/B-VII.1 data extracted from the OECD/Janis database for the most critical diluent reactions, as compared with the capture XS from U-238. Palladium isotopes display relatively high capture cross-sections, those are responsible for lower K-effective of 1,411 pcm. Molybdenum capture cross-sections are also relatively large and they impact the neutron balance by 1,651 pcm. In the case of the MTZ

diluent, the weight fraction from Zr is reduced, inserting 877 pcm of reactivity, while Ti addition reduces the K-effective by 653 pcm. In fact, Ti-48 was found to have a large impact on the neutron spectrum of the SFR due to its very large elastic scattering resonances in the epithermal energy range. This resonance from Ti-48 was identified as the main responsible for the reduced spectrum in the 15-100 keV energy range and increased low-energy tail observed in Figure 2.

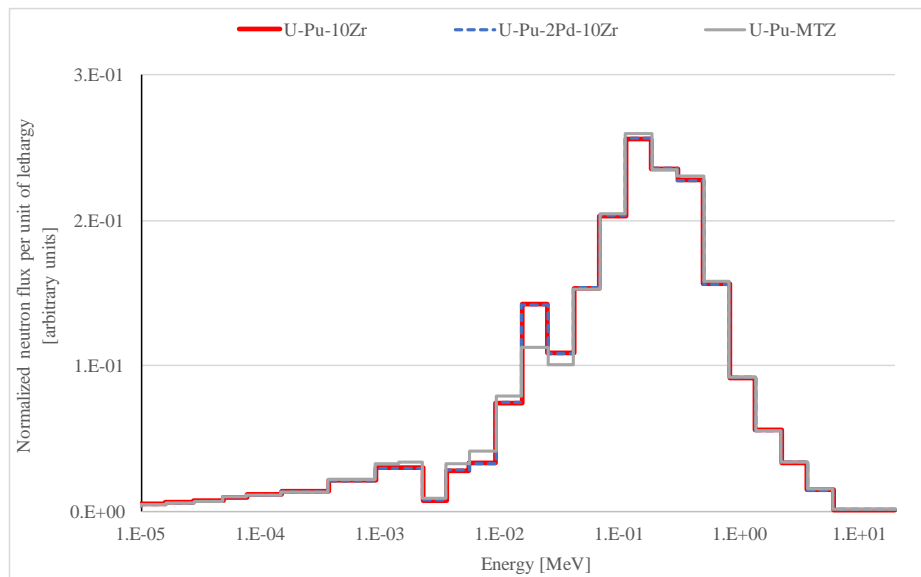


FIG. 2. Comparison of the neutron flux spectra with different transmutation fuels.

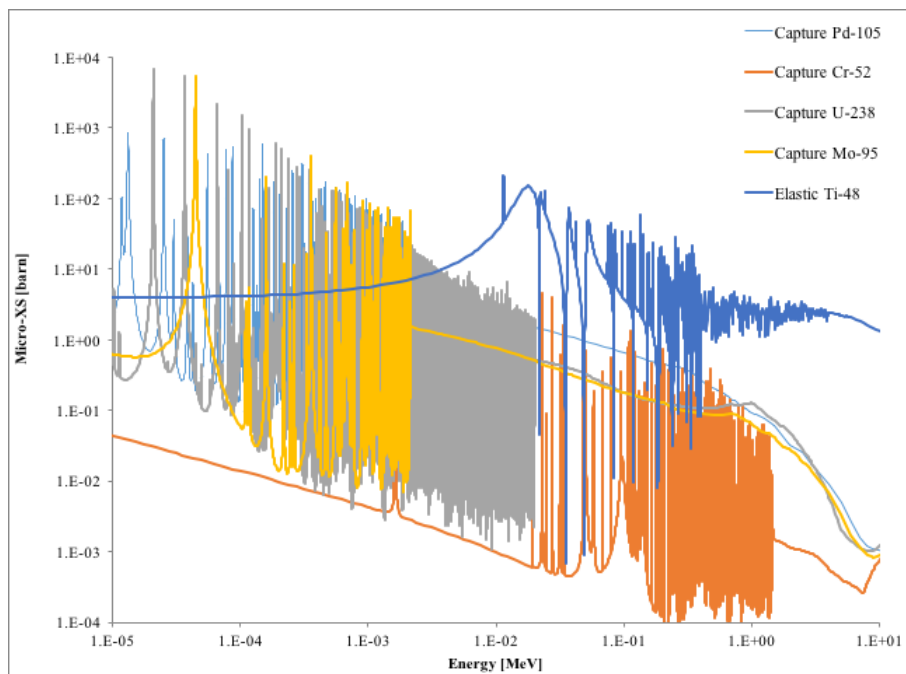


FIG. 3. Comparison of cross-sections between U-238, Cr-52, Mo-95, Pd-105 and Ti-48.

### 3. Impact of Advanced Fuels on SFR characteristics at equilibrium

Neutronic calculations were performed with the ANL suite of Fast Reactor codes to characterize the equilibrium cycle of the ABR-1000 concept using the above described advanced metallic fuel options. The main reactor physics parameters compared in Table V are

the conversion ratio (CR), the reactivity swing across the equilibrium cycle, the average fraction of TRU loaded in the core, the peak fast flux, the spectrum hardness, the delayed neutron fraction, the Doppler and the sodium void worth coefficients. The TRU content needed to sustain criticality throughout the cycle duration is being searched with REBUS-3. For complementary information, the isotopic compositions of the charged and discharged fuels are displayed in Table VI. For all calculations performed, the cycle length is calculated to reach the average discharged burnup of 100 GWd/t for all cases except with the U-Pu-4Pd-10Zr fuel where 200 GWd/t is targeted.

TABLE V: IMPACT OF TRANSMUTATION FUELS ON REACTOR PHYSICS PARAMETERS AT EQUILIBRIUM CYCLE.

Fuel Form	Cycle length EFPD <sup>3</sup>	$\Delta\rho_{\text{cycle}}$ pcm	Burnup avg. GWd/t	CR <sup>1</sup>	Avg. TRU %	Peak fast flux $10^{15}\text{n/cm}^2\text{-s}$	%E>0.1 MeV	$\beta_{\text{eff}}$ <sup>2</sup> pcm	$K_{\text{Dopp}}$ <sup>2</sup> \$	$\Delta\rho_{\text{void}}$ <sup>2</sup> \$
U-Pu-10Zr	394	2540	100	0.84	21.7%	3.4	67.2	335	-0.96	4.1
U-Pu-10Zr + Cr coating	389	2594	100	0.83	22.0%	3.4	67.2	334	-0.97	4.1
U-Pu-2Pd-10Zr	385	2878	100	0.80	23.4%	3.3	67.6	330	-0.83	4.5
U-Pu-2Pd-10Zr + Cr coating	380	2925	100	0.80	23.7%	3.3	67.6	329	-0.83	4.5
U-Pu-4Pd-10Zr	752	7921	200	0.69	31.6%	3.1	68.4	315	-0.54	5.0
U-Pu-4Pd-10Zr + Cr coating	743	7965	200	0.68	32.0%	3.1	68.3	314	-0.54	5.0
U-Pu-MTZ	370	3041	100	0.78	24.7%	3.2	68.4	328	-0.96	4.0
U-Pu-MTZ + Cr coating	366	3079	100	0.78	25.1%	3.2	68.3	327	-0.96	4.0
U-Pu-2Pd-MTZ	359	3306	100	0.75	26.7%	3.1	68.7	323	-0.83	4.3
U-Pu-2Pd-MTZ + Cr coating	354	3344	100	0.74	27.1%	3.1	68.6	322	-0.83	4.3

<sup>1</sup> CR stands for Conversion Ratio

<sup>2</sup> Parameters calculated at BOEC. For the  $\Delta\rho_{\text{void}}$ , 100% of the sodium in the driver fuel assembly is voided.

<sup>3</sup> Equivalent Full Power Day

TABLE VI: BREAKDOWN OF THE FUEL COMPOSITIONS AT CHARGE AND DISCHARGE.

	U-Pu-10Zr		U-Pu-10Zr +Cr coating		U-Pu-2Pd-10Zr		U-Pu-MTZ	
	charged	discharged	charged	discharged	charged	discharged	charged	discharged
Isotopic Composition [kg/cycle]								
U-238	2918.2	2615.4	2869.3	2573.6	2788.7	2511.6	2635.5	2379.1
Np-237	3.5	3.5	3.5	3.4	3.5	3.5	3.4	3.3
Pu-238	16.1	13.0	16.3	13.2	18.0	14.4	18.8	15.0
Pu-239	393.7	344.5	392.1	341.8	400.4	342.3	392.9	331.4
Pu-240	251.3	227.7	254.0	229.7	268.2	240.4	280.7	251.4
Pu-241	42.1	33.9	42.8	34.4	46.3	36.4	49.0	38.6
Pu-242	57.9	50.8	59.4	52.2	66.7	58.5	71.3	62.7
Am-241	17.4	13.9	17.7	14.2	19.4	15.6	20.3	16.3
Am-243	12.9	13.0	13.2	13.4	14.7	14.9	15.7	15.9
Cm-244	9.1	9.9	9.3	10.2	10.1	11.1	10.9	12.0
Cm-245	1.9	1.9	1.9	1.9	2.1	2.1	2.2	2.3
Cm-246	1.1	1.1	1.1	1.1	1.2	1.2	1.3	1.3
Fission Products	0.0	393.9	0.0	389.2	0.0	384.7	0.0	370.2
External Feed of Plutonium (from LWR)								
Pu [kg/EFPY <sup>1</sup> ]	31		32		37		40	

<sup>1</sup> Equivalent full power year

## 2.2 Impact of Palladium Addition

The addition of Palladium in the diluent of the fuel is found to significantly impact the neutronic characteristics of the SFR core at equilibrium. As observed in Table V both for the 10%Zr and MTZ types of fuels, adding 2wt% of Pd leads to increase the TRU content by about 2% (as also observed in Table VI), and a subsequent reduction in the breeding ratio by  $\sim 0.03$ , an increase in the burnup reactivity swing by  $\sim 300$  pcm/cycle and in the external feed of Pu from 31 kg to 37 kg per equivalent full power year. This external feed of plutonium is assumed to come from PWR and contains larger content of Pu-241 and decays into more Am-241, which explains the larger content of minor actinides in the 2%Pd fuel observed in Table VI. The addition of Palladium also affects the Doppler and the sodium void worth coefficients as shown in Table V.

An intermediate calculation was performed starting from U-Pu-10Zr fuel with reduced heavy nuclei density (consistent with that of 2%Pd addition) to de-correlate the effects from the changes in HN density and the addition of Palladium. The results summarized in Table VII show that both effects play a large impact on most of the reduced neutronic performance with Pd addition. The increased neutron absorption from Pd cross-section and subsequent higher TRU content leads to an increased spectrum hardening, which impacts the sodium void worth and the Doppler effect. The harder spectrum leads to increased spectral component for the sodium void worth coefficient. The reduction in the epithermal flux also reduces the Doppler coefficient (by 10-15% per 2%Pd addition).

The addition of 4wt% of Palladium is considered for higher burnup fuels. As a consequence, the results in Table V show the combined impacts from 4%Pd addition and from increasing the burnup target. Without increase in burnup target, the impact of 4wt% addition of Pd is about twice the impact observed with 2%Pd addition, and the TRU fraction would be 25%. The increase in fuel burnup leads to significantly increase the TRU content needed (up to 31.6%) to reach criticality throughout the cycle due to the relatively low conversion ratio and high reactivity swing. It should be noted that a reactivity swing of nearly  $\sim 8,000$  pcm is not very realistic for an SFR and would require to reduce the cycle length and increase the number of batches. This was not done in this analysis for consistency with other calculations and because this should not affect much the other neutronic parameters.

TABLE VII: BREAKDOWN OF THE IMPACT OF 2WT% PALLADIUM ADDITION ON REACTOR PHYSICS PARAMETERS.

	Cycle length EFPD	$\Delta\rho_{\text{cycle}}$ pcm	CR	Avg. TRU %	Peak fast flux $10^{15}\text{n/cm}^2\text{-s}$	%E>0.1 MeV	$\beta_{\text{eff}}$ pcm	$K_{\text{Dopp}}$ \$	$\Delta\rho_{\text{void}}$ \$
Reduction of HN density	-9	123	-0.01	0.7%	-0.01	0	-2	0.004	-0.1
XS changes from addition of 2%Pd	0	215	-0.02	1.0%	-0.11	0.4	-3	0.133	0.5
Total impact	-9	339	-0.03	1.7%	-0.12	0.4	-5	0.136	0.4

## 2.2 Impact of MTZ versus 10Zr

Replacing 10%Zr diluent by MTZ (5Mo-4.3Ti-0.7Zr) also leads to noticeable changes in the reactor physics parameters, as observed in Table V. When compared with the reference U-Pu-10Zr case, the TRU fraction is increased by 3% to reach criticality over the operating cycle of 370 EFPD. The reactivity swing is increased by 20% to about 3,000 pcm/cycle as the conversion ratio is reduced by 6%. The external feed of plutonium is increased from 31 kg to 40 kg per equivalent full power year, as observed in Table VI. The effects on the Doppler and sodium void worth coefficients are small and can be neglected. Like previously, those results



are the combination of two phenomena: the reduction of the HN density, and the changes in diluent cross-sections.

The relative contributions from changes in HN density and changes in cross-sections are observed in Table VIII. The reduction in HN density especially requires higher TRU content, which affects the conversion ratio and reactivity swing on a shorter cycle length. The different cross-sections between 10%Zr and MTZ affect the TRU content together with the flux level and spectrum as already observed in Figure 2. However, the change in neutron spectrum does not impact, in this particular case, the overall value of the Doppler and sodium void worth coefficients.

TABLE VIII: BREAKDOWN OF THE IMPACT OF MTZ VERSUS 10%ZR DILUENT ON REACTOR PHYSICS PARAMETERS.

	Cycle length EFPD	$\Delta\rho_{\text{cycle}}$ pcm	CR	Avg. TRU %	Peak fast flux $10^{15}\text{n/cm}^2\text{-s}$	%E>0.1 MeV	$\beta_{\text{eff}}$ pcm	$K_{\text{Dopp}}$ \$	$\Delta\rho_{\text{void}}$ \$
Reduction of HN density	-23	291	-0.03	1.7%	-0.01	0	-4	0.00	-0.2
XS changes from 10Zr to MTZ	0	210	-0.02	1.3%	-0.15	1.2	-3	0.00	0.1
Total impact	-23	501	-0.05	3.1%	-0.16	1.2	-7	0.00	-0.1

## 2.2 Impact of Chromium coating

As observed in Table V, a 20  $\mu\text{m}$  Chromium coating layer has a very small effect on the reactor physics parameters. The TRU content needed is slightly increased by  $\sim 0.3\%$  with small effects on the conversion ratio and reactivity swing. The content of Cr added through coating remains relatively small and the capture cross-sections of Cr isotopes are small as shown in Figure 3. Consequently, most of the effect observed is expected to come from the reduction in the initial radius of the fuel slug by  $\sim 20\ \mu\text{m}$  to maintain reference cladding dimensions and smeared density, which reduces the volume fraction of the fuel (after swelling) from 40.3% to 39.9%.

## 4. Conclusions and Summary

Advanced metallic fuels for Sodium-cooled Fast Reactors (SFR) are investigated to help mitigating the chemical interaction between the fuel and cladding, and to allow higher burnup. Different diluent materials such as Zirconium, MTZ (5Mo-4.3Ti-0.7Zr), with addition of 2-4 wt% of Palladium are considered, together with Cr-coating inside the cladding. This analysis assesses the design tradeoff in SFRs when using advanced transmutation fuels, based on the ABR-1000 core concept, and compared with the traditional U-Pu-10Zr fuel option used as a reference.

The changes in metallic fuel materials were confirmed to display a significant impact on the reactor physics parameters of an SFR, as summarized in Table IX, due to the reduction in heavy nuclei density and to the addition of more absorbing elements. A 2wt% addition of Palladium in the fuel leads to lower HN density and brings more absorbing materials, this is compensated by increasing the averaged TRU content by  $\sim 2\%$ . The reduced neutron flux in the low-energy range affects the neutronic feedback coefficients by reducing quite significantly the Doppler effect and increasing the sodium void worth. Such changes might require additional safety analysis to demonstrate the inherent safety of the reactor remains acceptable. Using MTZ diluent instead of 10%Zr also affects the reactor physics parameters due to lower HN density and more absorbing Mo isotopes, requiring an increase in averaged

TRU content by ~3%. In this case, however, no significant changes in the feedback coefficients were observed despite the large shift in neutron spectrum observed and associated with elastic scattering of Ti-48. A 20  $\mu\text{m}$  coating of Chromium was found to have a very minor effect on the reactor physics parameters.

TABLE IX. RELATIVE IMPACT OF FUEL CHANGES ON REACTOR PHYSICS PARAMETERS.

(Pert-Ref)/Ref, [%]	2wt% Pd addition	MTZ vs. 10Zr	20 $\mu\text{m}$ Cr coating
Cycle length	-2.3%	-5.9%	-1.2%
$\Delta\rho_{\text{cycle}}$	13.3%	19.7%	2.1%
Conversion ratio	-4.2%	-6.4%	-0.7%
Average TRU content	7.9%	14.2%	1.8%
Peak fast flux	-3.5%	-4.7%	-0.3%
Fast neutron fraction	0.6%	1.8%	0%
Delayed neutron fraction	-1.5%	-2.1%	-0.3%
Doppler constant	-14.1%	-0.3%	0.2%
Sodium void worth	9.5%	-1.9%	-0.5%

## Acknowledgement

Argonne National Laboratory's work was supported by U.S. Department of Energy (DOE) under Contract number DE-AC02-06CH11357. The direction and support of the U.S. DOE Office of Nuclear Energy is greatly appreciated.

## References

- [1] S. L. HAYES, "Advances in Metallic Fuels for High Burnup and Actinide Transmutation," Proceedings of the 14IEMPT conference, San Diego, CA, USA, Oct 17-20, (2016).
- [2] T. K. KIM, W. S. YANG, C. GRANDY, and R. N. HILL, "Core Design Studies for a 1000 MWth Advanced Burner Reactor," *Annals of Nuclear Energy*, Vol. 36, (2009).
- [3] S. L. HAYES, Personal Communication, 2016.
- [4] C. H. LEE and W. S. YANG, "Development of Multigroup Cross Section Generation Code MC<sup>2</sup>-3 for Fast Reactor Analysis," International Conference on Fast Reactors and Related Fuel Cycles, Kyoto, Japan, Dec. 7-11 (2009).
- [5] M. B. CHADWICK et al., "ENDF/B-VII.0: Next Generation Evaluated Nuclear Data Library for Nuclear Science and Technology," *Nuclear Data Sheets* 107, 2931 (2006).
- [6] K. L. DERSTINE, "DIF3D: A Code to Solve One-, Two-, and Three-Dimensional Finite Difference Diffusion Theory Problems," ANL-82-64, Argonne National Laboratory (1984).
- [7] G. PALMIOTTI et al., "Variational nodal transport methods with anisotropic scattering," *Nuclear Science and Engineering*, Vol. 115, pp. 233-243 (1993).
- [8] B. J. TOPPEL, "A User's Guide to the REBUS-3 Fuel Cycle Analysis Capability," ANL-83-2, Argonne National Laboratory (1983).

- [9] J. LEPPANEN, “Serpent – a Continuous-energy Monte Carlo Reactor Physics Burnup Calculation Code,” User’s Manual, June 18, (2015).
- [10] Benchmark for Neutronic Analysis of Sodium-cooled Fast Reactor Cores with Various Fuel Types and Core Sizes, OECD Nuclear Energy Agency, February 2016, NEA/NSC/R(2015)9.
- [11] C. H. LEE, N. E. STAUFF, “Improved Reactivity Worth Estimation of MC<sup>2</sup>-3/DIF3D in Fast Reactor Analysis,” Proceedings of ANS Sumer Meeting, paper 14201, San Antonio, Texas (2015).